Turkish Journal of Chemistry

Volume 46 | Number 4 Article 25

1-1-2022

Simulation of two electrode reactions coupled by the chemical reaction

MILIVOJ LOVRIC

TÜBİTAK

Turkish Journal of Chemistry

http://journals.tubitak.gov.tr/chem/

Research Article

Turk J Chem
(2022) 46: 1226-1233
© TÜBİTAK
doi:10.55730/1300-0527.3429

Simulation of two electrode reactions coupled by the chemical reaction

Milivoj LOVRIĆ*
Divkovićeva 13, Zagreb, Croatia

Received: 09.02.2022 • **Accepted/Published Online:** 11.04.2022 • **Final Version:** 05.08.2022

Abstract: A model of an ECE mechanism consisting of two reversible electrode reactions coupled by the kinetically controlled, second order, reversible chemical reaction is developed for the staircase cyclic voltammetry on the rotating disk electrode. The relationship between the limiting current of the second wave and the rate constant of chemical reaction is investigated. The concentration of electroinactive component of the forward reaction influences the half-wave potential of the first wave and the limiting current of the second wave. The responses of the mechanisms with reversible and irreversible chemical reactions are compared.

Key words: ECE mechanism, rotating disk electrode, staircase cyclic voltammetry, simulation, polarographic wave

1. Introduction

In organic electrolytes, electrode reactions of many compounds, such as catechols [1] and quinones [2], consist of two successive electron transfers connected by the transfer of protons [3–5]. These reactions are examples of the ECE mechanism [6–12] and the nine-member square scheme [13–15]. They were observed in electroreduction of p-nitrosophenol [16, 17], benzenesulfonyl floride [18, 19] and hexacyanochromate(III) [20] and in electrooxidation of tocopherols [21], methylcatechol [22, 23] and dopamine [24]. The theory of this mechanism is developed for polarography [8, 25–29], cyclic voltammetry [20, 30–33], square wave voltammetry [34–38], rotating disk measurements [39, 40] and the surface reactions in protein film voltammetry [41, 42]. The steady state responses on the rotating disk were calculated for totally irreversible chemical reactions and in this paper the investigation is extended to kinetically controlled, second order, reversible chemical reactions. The role of the electroinactive component of the reaction is analysed.

2. Model

It is assumed that an electrolytic solution contains dissolved reactant of the first electrode reaction and an electroinactive substance Y that cannot react with the mentioned reactant. The first electron transfer is fast and reversible electrooxidation. Its product cannot participate in the second electron transfer, but it can react with the substance Y to produce a compound that is stable at the given potential, but can be electrooxidized at higher potentials. Both chemical reaction and the second electrode reaction are reversible and the latter is fast. This mechanism can be represented by the following chemical equations:

$$A \leftrightarrow B + e^- \quad (1)$$

$$B + Y \leftrightarrow G \quad (2)$$

$$G \leftrightarrow H + e^- \quad (3)$$

On the rotating disk electrode, the mass transfer and currents are defined by the following system of differential equations and the initial and boundary conditions:

$$\frac{\partial c_A}{\partial t} = D\frac{\partial^2 c_A}{\partial x^2} - v\frac{\partial c_A}{\partial x} \quad (4)$$

$$\frac{\partial c_B}{\partial t} = D\frac{\partial^2 c_B}{\partial x^2} - v\frac{\partial c_B}{\partial x} - k_f c_B c_Y + k_b c_G \quad (5)$$

$$\frac{\partial c_Y}{\partial t} = D\frac{\partial^2 c_Y}{\partial x^2} - v\frac{\partial c_Y}{\partial x} - k_f c_B c_Y + k_b c_G \quad (6)$$

* Correspondence: milivojlovric13@gmail.com

$$\frac{\partial c_G}{\partial t} = D\frac{\partial^2 c_G}{\partial x^2} - v\frac{\partial c_G}{\partial x} + k_f c_B c_Y - k_b c_G \quad (7)$$

$$\frac{\partial c_H}{\partial t} = D\frac{\partial^2 c_H}{\partial x^2} - v\frac{\partial c_H}{\partial x} \quad (8)$$

$$t = 0, x \geq 0: c_A = c_A^*, c_B = 0, c_Y = c_Y^*, c_G = 0, c_H = 0 \quad (9)$$

$$t > 0, x \to \infty: c_A \to c_A^*, c_B \to 0, c_Y \to c_Y^*, c_G \to 0, c_H \to 0 \quad (10)$$

$$x = 0: \quad c_{B,x=0} = c_{A,x=0}\, exp\left(\frac{F}{RT}(E - E_1^0)\right) \quad (11)$$

$$c_{H,x=0} = c_{G,x=0}\, exp\left(\frac{F}{RT}(E - E_2^0)\right) \quad (12)$$

$$D\left(\frac{\partial c_A}{\partial x}\right)_{x=0} = \frac{I_1}{FS} \quad (13)$$

$$D\left(\frac{\partial c_B}{\partial x}\right)_{x=0} = -\frac{I_1}{FS} \quad (14)$$

$$\left(\frac{\partial c_Y}{\partial x}\right)_{x=0} = 0 \quad (15)$$

$$D\left(\frac{\partial c_G}{\partial x}\right)_{x=0} = \frac{I_2}{FS} \quad (16)$$

$$D\left(\frac{\partial c_H}{\partial x}\right)_{x=0} = -\frac{I_2}{FS} \quad (17)$$

$$v = -0.510\, \omega^{3/2} \nu^{-1/2} x^2 \quad (18)$$

$$K = \frac{k_f}{k_b}. \quad (19)$$

The meanings of all symbols are reported in Table. Equations (4)–(8) were solved by the finite difference method [43]. The current was calculated for the staircase cyclic voltammetry. The dimensionless current is defined by the following equations:

$$\Phi = (I_1 + I_2)\delta_{ss}/FSc_A^* D \quad (20)$$

$$\delta_{ss} = 1.61\, D^{\frac{1}{3}} \nu^{\frac{1}{6}} \omega^{-\frac{1}{2}}. \quad (21)$$

The following parameters were not changed: $D = 10^{-5}$ cm^2/s, $\nu = 10^{-2}$ cm^2/s, $\Delta t = 10^{-5}$ s, $\frac{D\Delta t}{\Delta x^2} = 0.2$, $\Delta E = 1$ mV and $\tau = 10$ ms.

Table. Meanings of symbols.

Symbol	Meaning
c_Z	Concentration of species Z
c_A^*, c_Y^*	Bulk concentrations of species A and Y
D	Diffusion coefficient
δ	Diffusion layer thickness
ΔE	Potential increment
Δt	Time increment
Δx	Space increment
E	Potential
E_1^0, E_2^0	Standard potentials
F	Faraday constant
I_1, I_2	Currents
ν	Kinematic viscosity
k_f, k_b	Rate constants of chemical reaction
K	Equilibrium constant of chemical reaction
ω	Rotation rate
R	Gas constant
S	Electrode surface area
t	Time
T	Temperature
τ	Step duration
v	Flow rate of solution

3. Results and discussion

On the rotating disk electrode, the cyclic staircase voltammograms of the ECE mechanism with stable intermediates depend on the scan rate, the electrode rotation rate and the kinetics of chemical reaction. Some examples are shown in Figure 1. They were calculated assuming that the concentration of substance Y can be freely changed and adjusted to the concentration of the reactant A. If the rate constants of chemical reaction are very high and equal ($Kc_A^* = 1$) and the rotation rate is low, the response is characterized by two maxima and two minima at 0.027 V, 0.378 V, 0.281 V, and –0.057 V vs. E_1^0, respectively. Considering that $E_2^0 - E_1^0 = 0.3$ V, the two parts of the response are well separated. The last minimum at –0.057 V is important because it shows that very fast chemical reaction is transforming the second reactant G into the first product B in the reverse branch of voltammograms. This minimum is the evidence that the whole ECE mechanism is close to the equilibrium. The absence of this minimum that can be noted in Figure 1B shows that chemical reaction is irreversible. It is a consequence of very high equilibrium constant and very low backward rate constant that cannot produce the first product B in the reverse branch. The potentials of two maxima and the minimum are: –0.058 V, 0.340 V, and 0.261 V, respectively. The potential of the first maximum is 85 mV lower than in Figure 1A because the chemical reaction is consuming the product of the first electrode reaction and decreasing the formal potential of the first electron transfer [33].

At higher rotation rates, the maxima and minima disappear and the response acquires the form of polarogram. The dimensionless limiting current of the first wave is equal to unit at 0.15 V vs. E_1^0. This is the base line for the measurement of limiting currents of the second wave. In Figure 1A the half-wave potentials are –0.019 V and 0.321 V in the anodic branch and –0.010 V and 0.330 V in the cathodic branch. This is because this response corresponds to the near steady state conditions. Under strict steady state both branches are overlapped. If $Kc_A^* = 10^3$ the first wave appears at –0.082 V because of irreversibility of chemical reaction.

Limiting currents of the second wave depend on the normalized forward rate constant of the chemical reaction. This is shown in Figure 2. The half-wave potentials of the second wave are changing from 0.298 V vs. E_1^0 ($k_f c_A^* = 1$ s^{-1}) to 0.321 V (curve 6) and those of the first wave from –0.004 V (1) to –0.019 V (6). These opposite trends are caused by the increasing rate of chemical reaction that creates a combination of EC and CE mechanisms. Furthermore, Figure 1A shows that the current at 0.8 V decreases with the increasing rotation rate. This is because the time that the product B spends near the electrode surface is longer if the rotation rate is slower. The limiting currents of the second wave depend on the logarithm of the product $k_f c_A^*$ in a sigmoidal manner, as can be seen in Figure 3. This figure also shows that the limiting currents of irreversible chemical reaction are higher than those of reversible one. Obviously, the backward component of the reaction diminishes its net gain. The relationship of this type can be represented by the general function [44]:

$$\Phi = 1 + \left(k_f c_A^*\right)^p / \left[\left(k_f c_A^*\right)^p + \left(k_f c_A^*\right)_{1/2}^p\right]. \tag{22}$$

Figure 4 shows that this representation is suitable for the limited range of the argument. The parameters $p$and $\left(k_f c_A^*\right)_{1/2}$ can be determined by the logarithmic analysis:

$$log\Psi = p\, log\left(k_f c_A^*\right) - p\, log\left(k_f c_A^*\right)_{1/2} \tag{23}$$

$$\Psi = (\Phi - 1) / [1 - (\Phi - 1)]. \tag{24}$$

Firstly the function Ψ is calculated and then the parameters are measured from the relationship between $log\Psi$ and $log\left(k_f c_A^*\right)$. For instance, the limiting currents shown by the curve 2 in Figure 3 when transformed by Eq. (24) gave a set of log values that depended linearly on the corresponding $\log(k_f c_A^*)$ arguments, with the slope 0.5 and the intercept 5.8 (not shown). The curves 1 and 2 in Figure 4 are defined by the following functions:

$$\Phi = 1 + \left(k_f c_A^*\right)^{0.4} / \left[\left(k_f c_A^*\right)^{0.4} + 54.54^{0.4}\right] \tag{25}$$

$$\Phi = 1 + \sqrt{k_f c_A^*} / \left[\sqrt{k_f c_A^*} + \sqrt{33.34}\right]. \tag{26}$$

This procedure is useful for the transformation of the set of discrete data into a continuous function. By the variation of concentrations of A and Y, keeping them equal, one can estimate the parameter p from the gradient $\partial log\Psi/\partial log c_A^*$. If the limiting current of the second wave is one half of the first limiting current and ω=40π rad /s, then logΨ=0 and $logk_f = log44 - log(c_A^*)_{1/2}$. The number 44 is an average of $\left(k_f c_A^*\right)_{1/2}$ values corresponding to reversible and irreversible chemical reactions. However, this estimation is rough and requires that the concentration of Y can be freely changed, which does not have to be fulfilled.

The variation of the bulk concentration of the substance Y influences both waves of the ECE response. The limiting current of the first wave is independent of but the half-wave potential of this wave decreases significantly with the increasing of this concentration. Regarding the second wave, its limiting current is influenced mostly, while $E_{1/2,2}$ is less affected. This is shown in Figure 5 for the reversible chemical reaction. The compound Y contributes to the forward rate of chemical reaction and its influence depends on the product $k_f c_A^*$. The relationship between $E_{1/2,1}$ and log (c_Y^*/c_A^*) is sigmoidal and in the vicinity of inflexion points it can be approximated by the straight lines:

$$E_{1/2,1} - E_1^0 = -0.029 \log (c_Y^*/c_A^*) + 0.018 \text{ V} \quad (27)$$

$$E_{1/2,1} - E_1^0 = -0.035 \log (c_Y^*/c_A^*) - 0.016 \text{ V}. \quad (28)$$

If the dimensionless equilibrium constant is 10^3 this relationship is very similar and the straight lines are:

$$E_{1/2,1} - E_1^0 = -0.028 \log (c_Y^*/c_A^*) + 0.015 \text{ V} \quad (29)$$

$$E_{1/2,1} - E_1^0 = -0.024 \log (c_Y^*/c_A^*) - 0.044 \text{ V}. \quad (30)$$

They apply for $k_f c_A^*$ 1 s^{-1} and 100 s^{-1}, respectively. The limiting currents of the second wave are the sigmoidal function of log (c_Y^*/c_A^*) if $k_f c_A^*$ 1 s^{-1}, but this relationship is only an upper fraction of the sigmoidal curve if 100 s^{-1}. This is because these two arguments add up giving the joint effect. If $Kc_A^* = 10^3$ the second half-wave potential is independent of c_Y^*, but if $Kc_A^* = 1$ it changes from the values reported in Figure 2 to 0.296 V vs. E_1^0, which is the potential that corresponds to the irreversible chemical reaction. This change occurs within the interval $1 < c_Y^*/c_A^* < 50$.

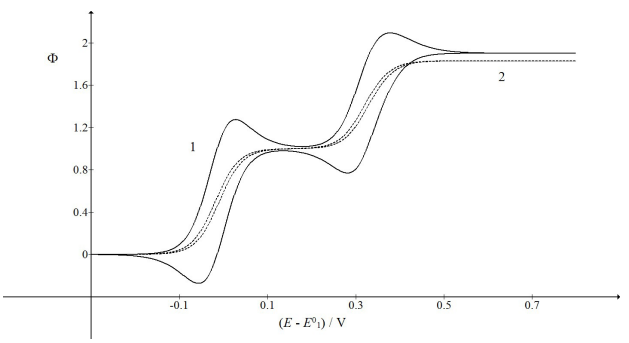

Figure 1A

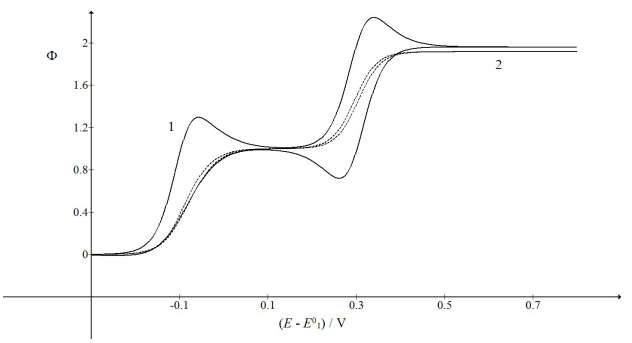

Figure 1B

Figure 1. Dimensionless cyclic staircase voltammograms of the ECE mechanism on the rotating disk electrode under the transient (full line) and near steady-state (broken line) conditions. $E_2^0 - E_1^0 = 0.3$ V, $\Delta E/\tau = 0.1$ V/s, $c_Y^*/c_A^* = 1$, $k_f c_A^* = 10^4$ s^{-1}, $Kc_A^* = 1$ (A) and 10^3 (B) and ω / rad $s^{-1} = 4\pi$ (1) and 40π (2).

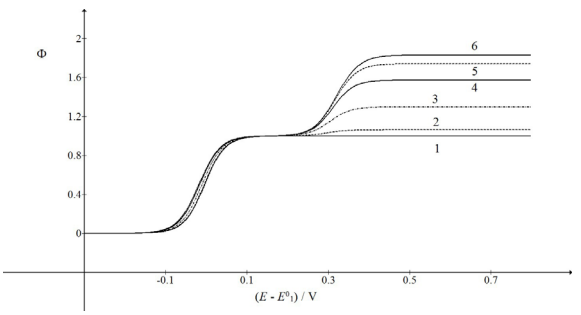

Figure 2. Dependence of the second wave on the product of the forward rate constant of chemical reaction and the bulk concentration of the reactant A. $Kc_A^* = 1$, $\omega = 40\pi$ rad/s and $k_f c_A^*$ / $s^{-1} = 0$ (1), 1 (2), 10 (3), 100 (4), 1000 (5) and 10000 (6). All other data are as in Figure 1.

The difference in limiting currents of the second wave between the ECE mechanisms with reversible and irreversible chemical reactions can be explained by the inspection of distribution of chemical species in the diffusion layer that is shown in Figure 6. One can notice that the dimensionless concentrations of B, Y and G are particularly sensitive to the dimensionless equilibrium constant of chemical reaction. If the reaction is reversible the concentration of Y at the electrode surface is 0.26 and the maximum concentration of G is 0.05, but under the influence of irreversible reaction these concentrations change to 0.17 and 0.1, respectively. Consequently, the gradient of H is steeper if the reaction is irreversible and the current is higher.

The models of ECE mechanism in the voltammetry on stationary macroelectrodes give qualitative descriptions of the responses because the transient currents consist of the diffusion and kinetic components [25, 33, 34, 38]. Under steady-state conditions on microelectrodes [6] and rotating disk electrodes [40] the diffusion component can be controlled and the kinetic contribution can be quantified. In this paper, it is shown that the kinetic current satisfies a general equation (22) and that the rate constant of chemical reaction can be estimated under certain conditions.

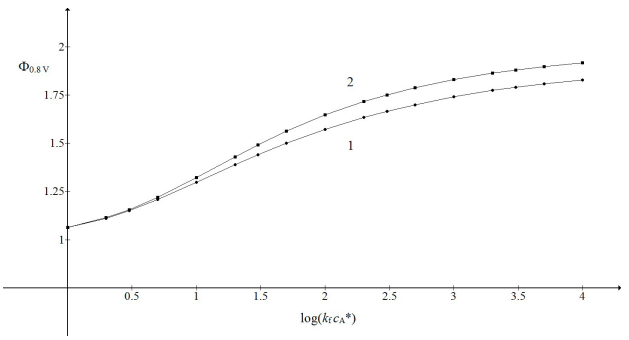

Figure 3. Dependence of the limiting current of the second wave on the logarithm of the product $k_f c_A^*$. $Kc_A^* = 1$ (1) and 10^3 (2). All other data are as in Figure 2.

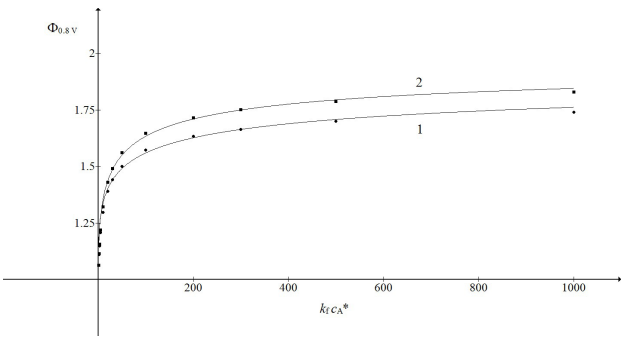

Figure 4. Dependence of the limiting currents of the second wave (the symbols) on the product $k_f c_A^*$. $Kc_A^* = 1$ (1) and 10^3 (2). The lines 1 and 2 are calculated by Eq. (22) using parameters p = 0.4 and $(k_f c_A^*)_{1/2}$ = 54.54 (1) and p = 0.5 and $(k_f c_A^*)_{1/2}$= 33.34 (2). All other data are as in Figure 2.

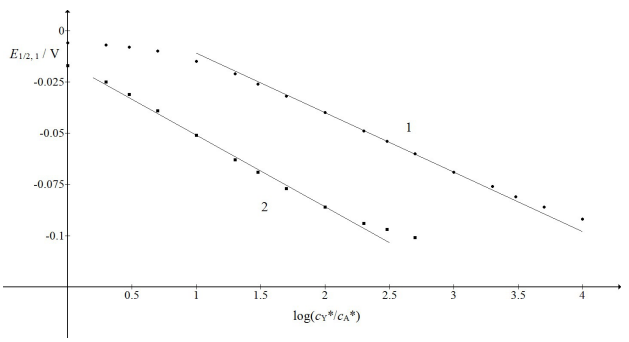

Figure 5A

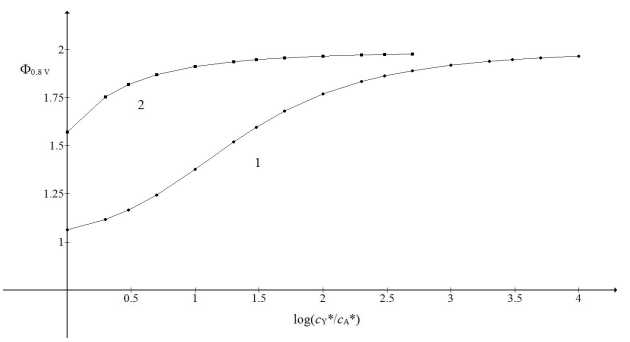

Figure 5B

Figure 5. Dependence of the half-wave potential of the first wave (A) and the limiting current of the second wave (B) on the logarithm of the ratio between bulk concentrations of the substance Y and the reactant A; $k_f c_A^*$ / s^{-1} = 1 (1) and 100 (2). The straight lines 1 and 2 are defined by Eqs. (27) and (28), respectively. All other data are as in Figure 2.

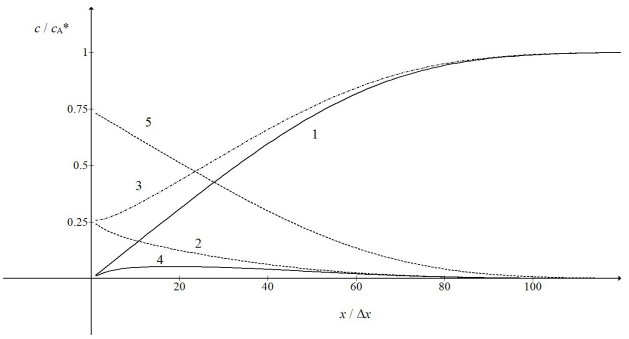

Figure 6A

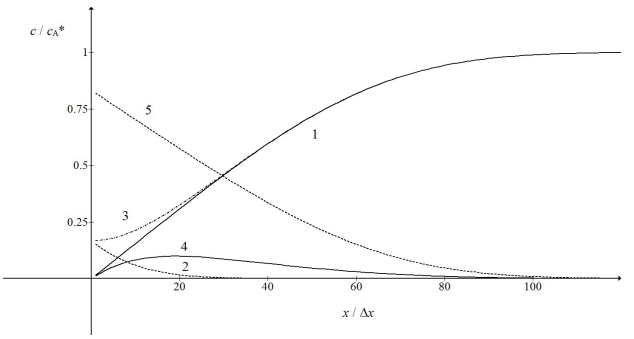

Figure 6B

Figure 6. Distribution of the reactant A (1), the product B (2), the compound Y (3), the second reactant G (4) and the final product H (5) in the diffusion layer at 0.8 V vs. E_1^0; ω= 40 rad/s, c_Y^*/c_A^* =1, $k_f c_A^*$ 10^3 s^{-1} and Kc_A^* = 1 (A) and 10^3 (B). All other data are as in Figure 1.

4. Conclusion

The difference between ECE mechanisms with the reversible and irreversible chemical reactions originates from the influence of the backward rate constant on the net gain of the reaction. If the reaction is of the second order, its forward rate depends on the component Y and the limiting current of the second wave becomes higher if the concentration of Y is increased. The rate constant can be estimated from the relationship between currents and the concentrations of the reactant of the first electrode reaction.

Dedication

Dedicated to the memory of Dr. Šebojka Komorsky-Lovrić.

Conflict of interest

The author declares no conflict of interest.

Data availability

All relevant data are available on demand.

References

1. Lin Q, Li Q, Batchelor-McAuley C, Compton RG. Two-electron, two-proton oxidation of catechol: kinetics and apparent catalysis. The Journal of Physical Chemistry C 2015; 119 (3): 1489-1495. doi: 10.1021/jp511414b
2. Gulaboski R, Markovski V, Jihe Z. Redox chemistry of coenzyme Q – a short overview of the voltammetric features. Journal of Solid State Electrochemistry 2016; 20 (12): 3229-3238. doi: 10.1007/s10008-3230-7
3. Wawzonek S, Berkey R, Blaha EW, Runner ME. Polarographic studies in acetonitrile and dimethylformamide. III. Behavior of quinones and hydroquinones. Journal of the Electrochemical Society 1956; 103 (8): 456-459.
4. Kolthoff IM, Reddy TB. Polarography and voltammetry in dimethylsulfoxide. Journal of the Electrochemical Society 1961; 108 (10): 980-984.
5. Peover ME. A polarographic investigation into the redox behaviour of quinones: the roles of electron affinity and solvent. Journal of the Chemical Society 1962; 4540-4549.
6. Molina A, Laborda E, Gomez-Gil J, Martinez-Ortiz F, Compton RG. A comprehensive voltammetric characterisation of ECE processes. Electrochimica Acta 2016; 195: 230-245. doi: 10.1016/elecacta.2016.01.120
7. Feldberg SW. Nuances of the ECE mechanism. III. Effects of homogeneous redox equilibrium in cyclic voltammetry. The Journal of Physical Chemistry 1971; 75 (15): 2377-2380. doi: 10.1021/j100684a025
8. Amatore C, Saveant JM. Do ECE mechanisms occur in conditions where they could be characterized by electrochemical kinetic techniques? Journal of Electroanalytical Chemistry and Interfacial Electrochemistry 1978; 86 (1): 227-232. doi: 10.1016/S0022-0728(78)80371-4
9. Palys MJ, Bos M, van der Linden WE. Automatic polarographic elucidation of electrode mechanisms by means of a knowledge-based systems: Part 3. Mechanisms ECE, EE and mechanisms involving adsorption. Analytica Chimica Acta 1993; 283 (2): 811-829. doi: 10.1016/0003-2670(93)85296-V

10. Sanecki PT, Amatore C, Skital PM. The problem of the accuracy of electrochemical kinetic parameter determination for the ECE reaction mechanism. Journal of Electroanalytical Chemistry 2003; 546: 109-121. doi: 10.1016/S0022-0728(03)00138-4

11. Sanecki PT, Skital PM. The mathematical models of kinetics of the E, EC, ECE, ECEC, ECE-ECE and ECEC-ECEC processes with potential-dependent transfer coefficient as a rationale of isoalpha points. Electrochimica Acta 2008; 53 (26): 7711-7719. doi: 10.1016/elecacta.2008.05.023

12. Gulaboski R, Mirčeski V, Bogeski I, Hoth M. Protein film voltammetry: electrochemical enzymatic spectroscopy. A review on recent progress. Journal of Solid State Electrochemistry 2012; 16 (7): 2315-2328. doi: 10.1007/s10008-011-1397-5

13. Laviron E, Mounier-Prest R. Electrochemical reactions with protonations at equilibrium: Part 14. The cubic scheme. Journal of Electroanalytical Chemistry 1992; 324: 1-18. doi: 10.1016/0022-0728(92)80032-Y

14. Molina A, Laborda E, Gomez-Gil JM, Compton RG. Staircase, cyclic and differential voltammetries of the nine-member square scheme at microelectrodes of any geometry with arbitrary chemical stabilization of the three redox states. Journal of Solid State Electrochemistry 2016; 20 (12): 3239-3253. doi: 10.1007/s10008-016-3308-2

15. Laborda E, Gomez-Gil JM, Molina A. Microelectrode voltammetry of multi-electron transfers complicated by coupled chemical equilibria: a general theory for the extended square scheme. Physical Chemistry Chemical Physics 2017; 19: 16464-16476. doi: 10.1039/C7CP02135F

16. Nicholson RS, Shain I. Experimental verification of an ECE mechanism for the reduction of p-nitrosophenol using stationary electrode polarography. Analytical Chemistry 1965; 37 (2): 190-195. doi: 10.1021/ac60221a003

17. Alberts GS, Shain I. Electrochemical study of kinetics of a chemical reaction coupled between two charge transfer reactions. Potentiostatic reduction of p-nitrosophenol. Analytical Chemistry 1963; 35 (12): 1859-1866. doi: 10.1021/ac60205a019

18. Sanecki P, Kaczmarski K. The voltammetric reduction of some benzenesulfonyl fluorides, simulation of the ECE mechanism and determination of the potential variation of the transfer coefficient by using the compounds with two reducible groups. Journal of Electroanalytical Chemistry 1999; 471 (1): 14-25. doi: 10.1016/S0022-0728(99)00243-0

19. Sanecki P, Skital P, Kaczmarski K. Numerical modelling of ECE-ECE and parallel EE-EE mechanisms in cyclic voltammetry. Reduction of 1,4-benzenedisulfonyl difluoride and 1,4-naphthalenedisulfonyl difluoride. Electroanalysis 2006; 18 (10): 981-991. doi: 10.1002/elan.200603487

20. Feldberg SW, Jeftić Lj. Nuances of the ECE mechanism. IV. Theory of cyclic voltammetry and chronoamperometry and the electrochemical reduction of hexacyanochromate(III). The Journal of Physical Chemistry 1972; 76 (17): 2439-2446. doi: 10.1021/j100661a017

21. Wilson GJ, Lin CY, Webster RD. Significant difference in the electrochemical behaviour of the α-, β-, γ- and δ- tocopherols (Vitamin E). The Journal of Physical Chemistry B 2006; 110 (23): 11540-11548. doi: 10.1021/jp0604802

22. Adams RN, Hawley MD, Feldberg SW. Nuances of the E. C. E. mechanism. II. Addition of hydrochloric acid and amines to electrochemically generated o-benzoquinones. The Journal of Physical Chemistry 1967; 71 (4): 851-855. doi: 10.1021/j100863a011

23. Nematollahi D, Golabi SM. Investigation of the electro-methoxylation reaction: Part 1. Electrochemical study of 4-tert-butylcatechol and 3,4-dihydroxybenzaldehyde in methanol. Journal of Electroanalytical Chemistry 2000; 481 (2): 208-214. doi: 10.1016/S0022-0728(99)00500-8

24. Li Y, Liu M, Xiang C, Xie Q, Yao S. Electrochemical quartz crystal microbalance study of growth and property of the polymer deposit at gold electrode during oxidation of dopamine in aqueous solutions. Thin Solid Films 2006; 497: 270-278. doi: 10.1016/j.tsf.2005.10.048

25. Engblom SO, Myland JC, Oldham KB. Response of an ECE reaction to a potential leap. Analytical Chemistry 1994; 66 (19): 3182-3187. doi: 10.1021/ac00091a029

26. Hawley MD, Feldberg SW. Nuances of the ECE mechanism. I. Development of the theoretical relationship for chronoamperometry. The Journal of Physical Chemistry 1966; 70 (11): 3459-3464. doi: 10.1021/j100883a015

27. Galvez J, Molina A, Saura R, Martinez F. Dc polarography: current – potential curves with a parallel ECE mechanism: calculation of the rate constants of the chemical reaction. Journal of Electroanalytical Chemistry and Interfacial Electrochemistry 1981; 127: 17-35. doi: 10.1016/S0022-0728(81)80464-0

28. Kastening B. Polarographic theory for an ECE [electrochemical – chemical – electrochemical] mechanism. Analytical Chemistry 1969; 41 (8): 1142-1144. doi: 10.1021/ac60277a016

29. Sobel HR, Smith DE. Dc polarography: on the theory for the current – potential profile with an ECE mechanism. Journal of Electroanalytical Chemistry and Interfacial Electrochemistry 1970; 26: 271-284. doi: 10.1016/S0022-0728(70)80310-2

30. Mastragostino M, Nadjo L, Saveant JM. Disproportionation and ECE mechanisms – I. Theoretical analysis. Relationship for linear sweep voltammetry. Electrochimica Acta 1968; 13 (4): 721-749. doi: 10.1016/0013-4686(68)85007-8

31. Amatore C, Saveant JM. Ece and disproportionation: Part V. Stationary state general solution application to linear sweep voltammetry. Journal of Electroanalytical Chemistry and Interfacial Electrochemistry 1977; 85 (1): 27-46. doi: 10.1016/S0022-0728(77)80150-2

32. Nicholson RS, Shain I. Theory of stationary electrode polarography for a chemical reaction coupled between two charge transfers. Analytical Chemistry 1965; 37 (2): 178-190. doi: 10.1021/ac60221a002

33. Komorsky-Lovrić Š, Lovrić M. Theory of staircase cyclic voltammetry of two electrode reactions coupled by a chemical reaction. Bulgarian Chemical Communications 2019; 51 (3): 348-357. doi: 10.34049/bcc.51.3.4983

34. Mann MA, Helfrick Jr JC, Bottomley LA. Diagnostic criteria for identifying an ECE mechanism with cyclic square wave voltammetry. Journal of the Electrochemical Society 2016; 163 (4): H3101-H3109.

35. Miles AB, Compton RG. Simulation of square-wave voltammetry at a channel electrode: E, EC and ECE processes. Journal of Electroanalytical Chemistry 2001; 499: 1-16. doi: 10.1016/S0022-0728(00)00460-5

36. O'Dea JJ, Wikiel K, Osteryoung J. Square-wave voltammetry for ECE mechanisms. The Journal of Physical Chemistry 1990; 94 (9): 3628-3636. doi: 101021/j100372a049

37. Miles AB, Compton RG. Simulation of square-wave voltammetry: EC and ECE electrode processes. The Journal of Physical Chemistry B 2000; 104 (22): 5331-5342. doi: 10.1021/jp0006882

38. Komorsky-Lovrić Š, Lovrić M. Theory of square wave voltammetry of two reversible electrode reactions connected by the reversible chemical reaction. To Chemistry Journal 2019; 2: 142-153.

39. Karp S. Homogeneous chemical kinetics with rotating disk electrode. ECE mechanism. The Journal of Physical Chemistry 1968; 72 (3): 1082. doi: 10.1021/j100849a057

40. Umadevi R, Visuvasam J, Venugopal K, Rajendran L. Mathematical models for ECE reactions at rotating disk electrodes using homotopy analysis method. AIP Conference Proceedings 2020; 2277: 130013-1. doi: 10.1063/5.0025822

41. Gulaboski R. Surface ECE mechanism in protein film voltammetry – a theoretical study under conditions of square-wave voltammetry. Journal of Solid State Electrochemistry 2009; 13: 1015-1023. doi: 10.1007/s10008-008-0665-5

42. Gulaboski R, Kokoškarova P, Mitrev S. Theoretical aspects of several successive two-step redox mechanisms in protein-film cyclic staircase voltammetry. Electrochimica Acta 2012; 69: 86-96. doi: 10.1016/j.electacta.2012.02.086

43. Strutwolf J, Schoeller WW. Linear and cyclic sweep voltammetry at a rotating disk electrode. A digital simulation. Electroanalysis 1996; 8 (11): 1034-1039. doi: 10.1002/elan.1140081111

44. Lovrić M. Modelling electrocatalytic reactions on rotating disk electrodes. Russian Journal of Electrochemistry 2022; 58 (3): 202-209. doi: 10.1134/S1023193522030077